Tellus (1988), *40A*, 375–391

Structural determinism of equilibrated baroclinic waves in a two-layer model and equivalent barotropy

By BRIAN REINHOLD, *Department of Meteorology,* Arrhenius Laboratory, University of Stockholm, S-106 91 Stockholm, Sweden*

(Manuscript received 1 June 1987; in final form 29 January 1988)

ABSTRACT

The time-average structures, zonal flows, and energies of a 21 by 21 wave quasi-geostrophic two-level channel model in the absence of zonally inhomogeneous external forcing mechanisms such as topography are contrasted on the β- and f-planes for several different parameter sets. In all cases, the phase lag, as well as the amplitude, of the temperature component relative to the streamfunction field for the longer waves is considerably less on the β-plane than the f-plane. The zonal flow speeds are also considerably faster on the β-plane. The results are examined in the light of quasi-geostrophic turbulence and structural determinism, heat-transport efficiency/equilibration concepts of Reinhold. The analysis suggests that the equivalent barotropic arrangements of the large-scale atmospheric waves may be primarily a response to the quasi-linear influences of the spherical geometry on the structures of the disturbances, which then, in turn, influence the level of amplitude equilibration and zonal flow speeds.

1. Introduction

Observation of the atmospheric energy spectra reveals that the bulk of the statistically equilibrated total energy resides in the zonal flow components and the largest planetary scales (Boer and Shepherd, 1983; Baer, 1972, 1974). The structure of these energy-containing features tend, furthermore, to be equivalent barotropic (Deland, 1973; Dole, 1986; Gall et al., 1979; Lau, 1979), among others. Why this particular energy-spectra distribution of equivalent barotropic structures should arise in a system where the principal source of kinetic energy stems from the occurrence of baroclinic instability on the synoptic scales, is an issue of considerable importance in both practical and theoretical contexts.

Two contrasting concepts appear to provide a qualitative bound on the nature of this equilibration: linear instability theory and quasi-geostrophic turbulence theory. The former identifies a particular scale and structure that is "preferred" above all others (for a given dynamical system) which then amplifies most rapidly and attains maximum energy. (In mid-latitude atmospheric contexts, this favored disturbance is usually attributed to baroclinic instability.) On the other hand, the purely nonlinear scrambling processes of homogeneous, isotropic, energy and enstrophy conserving two-dimensional turbulence require that energy upscales, leading to a maximum level in the largest scale component of the system. (The properties and behaviors of two-dimensional turbulence and its relation to the atmosphere are well elucidated by Shepherd (1987) and Boer and Shepherd (1983); in addition they provide a host of references to the classical works in this field.) The atmosphere, however, appears to lie somewhere between these two extremes. First, both the transient and stationary energy components (see Fig. 1 of Boer and Shepherd (1983)) tend to peak at scales larger than that of the baroclinically most unstable scales with structures that become much more equivalent barotropic than that indicated by linear theory (Gall, 1976a; among several others).

* Contribution no. 582.

Second, the energy maximum of the transient disturbances does not reside at the largest scale, as required by turbulence theory, and any structure is, of course, unaccounted for. Third, the form of the spectra is inconsistent with both models (Shepherd, 1987; and above references). (The aforementioned contrasts between peak growth rates, fluxes, and energies are particularly well illustrated for a doubly-periodic, quasi-geostrophic, two-layer model in Figs. 9 and 10c of Haidvogel and Held (1980).)

On the other hand, it is not surprising that these idealized theories are unable to account for the equilibrated state of the atmosphere, as several of the assumptions imposed by the two theories are violated. Clearly, the linear dynamics of instability theory is a serious shortcoming, as no consistent means for stopping the exponential growth and attaining an equilibrium are provided. The turbulent model, on the other hand, must be able to take into account anisotropy, such as time-average zonal and or wavy flows and the β effect, inhomogeneity such as the geometrical constraints upon the planetary scale disturbances, and nonconservative processes such as multiple scales of preferred forcing and dissipation. In short, any phenomenon or process which demands order or structure and thereby defeats the random aspect of the motions upon which the theory is based, must be accounted for, which has also been pointed out by Rhines (1979) and Shepherd (1987).

How does one then account for the observed statistically equilibrated energy and structural distributions of the atmosphere? Salmon (1980), among others, emphasize the rôle of modified turbulence theory, and demonstrate that certain conditions which lie outside the assumptions of the theory, e.g., anisotropy and baroclinicity, do not erradicate its usefulness. For example, baroclinic instability is viewed as an energy source at a particular scale which cascades both barotropic and baroclinic enstropy downscale to an eventual wavenumber to the -3 inertial range, and barotropic energy upscale. The two-dimensional turbulence aspects of the spectra then appear at those scales sufficiently far from the baroclinic energy source. The inability of the energy to peak at the largest scale in the atmosphere is then attributed to the geometrical constraints of the planetary waves; there simply is not enough "room" in spectral space for full barotropic interactions to take place. In the oceans, however, the scale of baroclinic instability is relatively small (about 25 km) compared to the basin dimensions, and the geometrical constraints may not be so relevant. Salmon also notes that model runs with β exhibit structures that are significantly more barotropic in the largest scales than runs without β. This behavior is explained by the β-induced shift of baroclinic instability (and thus the energy input) to smaller scales, which allows more room in spectral space for the barotropic processes to develop and thus leads to reduced amounts of baroclinic energy.

However, as pointed out by Shepherd (1987), a great deal of the atmospheric energy distribution simply cannot be sensibly understood within the context of classical turbulence theory, the most obvious component being the occurrence of any stationary flow. However, an additional difficulty arises from the fluxes of energy and enstrophy due to coupled interactions between the stationary and transient components, which Shepherd (1987) estimates accounts for about half of the transient energy fluxes and, in fact, dominates the transient components at the largest scales. Those aspects of the flow Shepherd considers consistent with a turbulence description are due only to the nonlinear self-interactions within the transients themselves.

Shepherd's observations suggest that even the transient components of the atmospheric flow are in some sense well organized, with the emphasis upon stationary-transient wave interactions, which are more in line with the weather regime phenomenon (Reinhold and Pierrehumbert, 1982). Here it is suggested that the organization of the transient behavior pointed out by Shepherd, even in the absence of non-zonal stationary flow, occurs, in part, through structural determinism (Reinhold, 1986, hereafter referred to as R). Structural determinism refers to the situation where the dynamic processes *due to the presence of a time mean state* are driving the disturbances to a *fixed* specified structure. Such a process means that the flow is non-turbulent as the flow features are not structurally random but are organized into preferred configurations. Preferred configurations, in turn, imply preferred transports of heat and vorticity and other dynamical quantities between both waves and the zonal flows. In this sense, structural determinism appears to be in direct competition with the scrambling processes of isotropic homogeneous turbulence, or from another point of view, a compliment to the turbulence concepts, as structural determinism is *only* applicable in forced-dissipative systems. Thus, in those flow situations that are strongly structurally deterministic (e.g., intensely forced, asymmetrically damped systems with high-energy time mean states within which an arbitrarily specified disturbance evolves rapidly to its quasi-linearly equilibrated configuration, see R), the concepts of turbulence theory must be considerably modified, whereas in structurally indeterministic flows (unforced, inviscid) the properties expected from turbulence considerations should dominate.

The point of this work is to demonstrate that structural determinism perhaps plays an important rôle in establishing the statistically equilibrated structures of the atmosphere, in particular at large scales, which then has its consequences for the energy spectrum. The aim of this effort is to explain the tendency for equivalent barotropy and certain aspects of the approximate scale at which the maximum energy occurs. The following is proposed.

(a) The state of equilibrium due to the organized structures is determined to a large extent by a balance condition between the external driving and dissipation of the system and the transports due to the concomitant disturbances.

(b) The level of equilibrated energy in the various components is then determined by the efficiency of a given disturbance in accomplishing these transports in the balance required in (a), which is determined by the structures.

(c) More inefficient structures require greater amplitude to accomplish a given transport and thus equilibrate at higher amplitudes leading to greater energies, given that all else remains the same.

The theoretical grounds upon which these arguments are based are provided by the study of R. This analysis investigates the processes that determine the structures of unstable baroclinic disturbances and their consequent equilibration in perhaps the simplest idealized baroclinic geophysical flow system that can be constructed: a two-level, quasi-geostrophic, truncated spectral model retaining a single wave and zonal jet.

The conditions for equilibrium in this idealized model are determined by a balance between the direct thermal driving and dissipation of the zonal jet and the poleward heat-transport efficiency of the imbedded disturbance. The efficiency, in turn, is determined totally by the wave structure, which is, in itself, determined through "linear dynamics" depending upon the external parameters and the zonal jet. The physical conditions that provides the mathematical closure for the system is that the zonal jet and disturbance structure adjust such that a state of marginal instability is attained (a kind of baroclinic adjustment process as quoted by Stone (1978) and the first of Salmon's (1980) or Vallis' (1988) three equilibration schematics). The amplitude is then determined by the amount of poleward heat transport required for the aforementioned balance.

The advantage of this idealized system is that the rôle the various parameters play in the determination of the wave structures (and therefore the heat-transport efficiencies) can be understood in conceptual detail. Thus, those parameters which decrease the structural efficiency of the wave (the so-called traditionally stabilizing parameters such as β, and similar dispersive mechanisms such as horizontal shear in the jet, and dissipation) often lead to increases in the zonal jet and level of amplitude equilibration.

For example, in the one-wave model, as one departs from the wavenumber that is traditionally most unstable (which is the most efficient at extracting energy from the basic state as well as transporting heat poleward), the efficiency decreases and the equilibrated amplitude must increase to maintain a specified poleward heat transport. On the other hand, the lowering efficiency of the structure is unable to reduce the zonal shears as effectively, resulting in a zonal wind distribution which requires a smaller heat transport for balance. The two mitigating behaviors in the one-wave model then generate a nonlinearly equilibrated amplitude profile as a function of wavenumber which peaks at wavenumbers on both the long and short wave side of the traditionally most unstable disturbance, but not necessarily at the longest or shortest waves (which are most inefficient). Parameters such as the zonal driving, however, which do not effect the structures, act only to alter the wave amplitudes; the zonal jet and eddy perturbation structures remain the same.

In this one-wave system, the β parameter leads to an equivalent barotropization of the disturbances though the asymmetric influence of β upon the advections of the temperature and vorticity fields; an upstream tendency is induced in the vorticity field while the direct advection of temperature is unaffected. The vorticity field then propagates upstream relative to the temperature field mitigating the maximally-efficient 90° phase lag between the streamfunction and temperature components established by the remaining processes concomitant with baroclinic instability (discussed in detail in R). The magnitude of this influence upon the nonlinearly equilibrated state in going from the f-plane to the mid-latitude β-plane is remarkable. Even at the longest waves, which are generally considered to be most barotropic in the atmosphere, the vertical phase tilts of the one-wave model equilibrated structures in the absence of β are pronounced. The reduced efficiencies in the poleward transport of heat by the β-induced equivalent barotropization simultaneously lead to marked increases in the zonal jet.

The robustness of this result in this model, as well as slightly higher resolution versions, suggests that the same phenomenon could perhaps be responsible for the equivalent barotropic structure of the large scale atmosphere, which invokes a different mechanism than that suggested by Salmon (1980) or implied by Gall (1976b) and Simmons and Hoskins (1978, 1980). However, the simplicity of the model considered in R does not allow one to draw any direct conclusions about the relation between spherical geometry or the β effect and the equivalent barotropic structures of more complicated flows or the atmosphere. The host of nonlinear interactions present in such systems could easily swamp the dynamical processes elucidated in the simple model. Basic feedback mechanisms such as momentum transports and wave-wave interactions are lacking in the idealized case. Clearly, the analysis of a more sophisticated system is required in order to test to what extent the processes identified in the idealized theory are still present in more realistic flows.

To accomplish this goal, a set of experiments on the f-plane and the β-plane are conducted in a model identical to the model of R, except that the degrees of freedom have been increased to contain 21 wavenumbers in both the zonal and meridional directions. The equilibrated structures, spectra, and zonal flows are then contrasted between the f-plane and β-plane cases, as well as with those structures anticipated by the one-wave theories. Further comparison with the atmosphere is, of course, limited, not only by the resolution, but also by the exclusion of other physical processes such as orography, which Li et al. (1986) have shown to have an important influence upon the statistically equilibrated spectra in laboratory experiments.

We must furthermore add that the simple model of R cannot fully explain the rôle of structural determinism in equilibration. It does not take into account any organization between the waves, such as those pointed out by Shepherd or the weather regime process; in other words, organization in the second equilibration mechanism of Salmon and Vallis (well elucidated by the latter). The one-wave model *only* describes the equilibration processes present in wave-mean flow interactions in forced-dissipative systems, such as Vallis' (1988) or Mak's (1985) multi-scale model where wave-wave interactions are explicitly removed (and thus eventually equilibrate to that single wave which has minimum critical shear). A more complete understanding of the rôle of structural determinism in the establishment of statistical equilibrium requires an understanding of what determines the structures in zonally inhomogeneous flows, which is extremely complicated even in the simplest of such systems.

Nevertheless, some of the influences upon equilibration due to the structural organizations discussed in the one-wave model appear to be sufficiently strong that they are still present in fully nonlinear forced-dissipative systems, in particular, the barotropization by β and the location of the energy maxima near the marginal curve of the *time mean* flows.

2. The model

The mid-latitude atmosphere is simulated in this study by a two-level, quasi-geostrophic, periodic β-plane channel model. The width of the channel is given by πL, where $y = 0$ denotes the subtropical boundary and $y = \pi L$ denotes the polar boundary. Defining ψ as the mean (barotropic) streamfunction, τ as the mean shear (baroclinic) streamfunction, θ as the mean potential temperature, and χ as the (divergent) velocity potential, the system of dynamical equations can be expressed by

$$\partial \nabla^2 \psi/\partial t + J(\psi, \nabla^2 \psi) + J(\tau, \nabla^2 \psi) + \beta \partial \psi/\partial x = k'' \nabla^2(\tau - \psi) - j'' \nabla^2(\tau + \psi),$$

$$\partial \nabla^2 \tau/\partial t + J(\psi, \nabla^2 \tau) + J(\tau, \nabla^2 \psi) + \beta \partial \tau/\partial x - f \nabla^2 \chi = -k'' \nabla^2(\tau - \psi) - 2k''' \nabla^2 \tau - j'' \nabla^2(\tau + \psi),$$

$$\partial \theta/\partial t + J(\psi, \theta) - \sigma \nabla^2 \chi = h'(\theta^* - \theta),$$

where $J(A, B)$ is the Jacobian operator $\partial A/\partial x\, \partial B/\partial y - \partial A/\partial y\, \partial B/\partial x$. The remaining seven quantities k'', j'', k''', β, h', σ, and θ^* correspond to the parameterized physical processes incorporated in the model. The first three, k'', j'', and k''', are the coefficients of Ekman dissipation on the vorticity field at the lower layer, upper layer, and between layers, respectively. Thermal damping is accomplished by Newtonian cooling on the temperature field whose intensity is denoted by h'. The system is driven thermally by a prescribed radiative equilibrium temperature field, denoted by θ^*, which is selected to have $\cos(y/L)$ structure, which, in the absence of instability, would drive a zonally symmetric baroclinic jet with a maximum intensity at the center of the channel. The static stability σ is assumed to be constant, while β, the meridional gradient of the coriolis force, is chosen to correspond to either mid-latitude values or zero. No sources of external zonal inhomogeneity (such as topography) or time variations (such as a diurnal or seasonal cycle) are imposed.

The system of equations is closed by the two-level model thermal wind relation

$$\nabla^2 \tau = (R/f) \ln(p_3/p_2) \nabla^2 \theta,$$

where p_2 and p_3 are the pressures at the center and lower layers, respectively, and R is the gas constant.

The equations are non-dimensionalized in space by the channel-width length scale L, in time by the coriolis parameter f, while the temperature is scaled through the thermal wind relation by the quantity $A = f/R \ln(p_3/p_2)$ and the scaled β parameter is given by the ratio of the length scale L and the radius of the earth. For typical values, f is chosen to be 10^{-4} s^{-1} and $\pi L = 5000$ km.

The system is then expanded into spectral eigenfunctions of the Laplace operator. The customary boundary conditions of no flow through the walls (which requires that the meridional velocity is zero at the walls) and no net drag upon the walls, combined with the channel geometry, determine the final form of the eigenfunctions which are a limited subset of the two-dimensional trigonometric functions. Wave modes (in non-dimensional form) are given by

$$F_{ml} = 2 \cos mnx \sin ly, \quad F'_{ml} = 2 \sin mnx \sin ly,$$

whereas zonal modes are given by

$$F_l = \sqrt{2} \cos ly,$$

where m and l are integer wavenumbers in the zonal and meridional directions, respectively. The parameter n measures the ratio of the largest scale in the meridional direction to the gravest mode in the zonal direction, and thus determines the largest scale allowed in the model. With the selected channel width of 5000 km, a value of $n = 0.35$ corresponds approximately to global wavenumber 1 at 45° latitude.

In the absence of any motion, the temperature distribution would assume that given by the radiative equilibrium value, while in the absence or suppression of instability, the zonally symmetric "Hadley solution" (Lorenz, 1963) ensues. The latter is easily obtained analytically by solving for the equilibrium in the absence of any wave motions (thus there is no advection). Other solutions must resort to numerical methods.

Numerical integrations utilize the transform technique, i.e., all space derivatives are calculated in Fourier space while the multiplications of the nonlinear Jacobian terms are carried out in grid point space and then transformed back into Fourier space (Orszag, 1970; Machenhauer and Rasmussen, 1972; Washington and Parkinson, 1986). The method is not completely straightforward, however, due to the boundary conditions imposed by the channel walls (see Vallis (1985)).

Except for the truncation, the spectral model considered here is identical to that of R, and for details, the reader is referred to that paper. For a more general and concise treatment of the mathematical development of the spectral equations, the reader is referred to Lorenz (1963).

3. Experiments

The level of truncation of the above model is set to 21 waves in both the zonal and meridional directions. Each run begins from an initial state of small-amplitude random perturbations in all wave components superimposed upon a zonal basic state of 22.5 $\mathrm{m\,s^{-1}}$ at mid-level and zero at the lower level. Integrations are carried out for 24,000 time steps or 640 days. Since the flows generated in these runs do not obtain a steady level of equilibration as in the nonlinear model of R, the state of statistical equilibrium (approximated by the time average) is utilized for comparisons. These time-average structures are computed by evaluating at each time step, for each two-dimensional wavenumber, the amplitude of, and the phase difference between, the streamfunction and potential temperature components, and averaging over the last 590 days of the run. (The first 50 days are set aside to allow the model to settle into its attractor.) There is, of course, always the problem of being able to estimate the "actual" state of statistical equilibrium due to the limited sample size. However, the smoothness of the structural and energy-spectra statistics obtained as a function of the parameters, and the fact that the characteristic variations of the energy fields are much shorter than the total integration time, suggests that a reasonable estimate of the aforementioned statistics is provided.

A total of 36 different parameter sets is chosen; three levels of dissipation, denoted by LF, MF, and HF (low, medium, and high friction, respectively) for three levels of driving, denoted by LD, MD, and HD (low, medium, and high driving, respectively) for two values of the static stability parameter, LS and HS (low and high, respectively), with and without β. The parameter n is set to 0.35 in all cases, which corresponds to global wavenumber 1 at 45° latitude.

The values of the parameters in dimensional and non-dimensional form are given in Table 1. The abbreviations used to name the parameter sets will also be used to identify experiments in the figures. In addition, two experiments are run with and without β in the absence of dissipation.

Table 1. *Parameters used for the experiments*

Dissipation:	Surface	Between-layer	Upper layer	Thermal
high:	2.9 days	23.1 days	none	2.6 days
HF	(0.04)	(0.005)	(0.0)	(0.045)
medium:	5.8 days	115.7 days	none	5.8 days
MF	(0.02)	(0.001)	(0.0)	(0.02)
low:	11.6 days	none	none	11.6 days
LF	(0.01)	(0.000)	(0.0)	(0.01)

static stability:

high:	46.3 K/500 mb	low:	30.9 K/500 mb
HS	(0.15)	LS	(0.10)

thermal driving (radiative equilibrium temperature difference):

high:	52.4°K	medium:	41.5°K	low:	30.5°K
HD	(0.12)	MD	(0.095)	LD	(0.07)

Beta: either zero or mid-latitude value (0.25 non-dimensional)

HF, MF, LF correspond to high, medium, and low friction. HD, MD, LD correspond to high, medium and low drivings. HS and LS denote high and low static stabilities. These abbreviations are used in the figures.

4. Results

The structures of the disturbances in spectral space can be entirely represented for each component by the amplitude ratio between the thermal (baroclinic) and streamfunction (barotropic) components (Q in the notation of R) and the phase difference between the stream-function and temperature fields (G in the notation of R). The poleward heat transport efficiency for that component is then proportional to $Q \sin G$. With this convention, more barotropic-type structures are given by values of Q and G approaching zero, while more baroclinic-type structures are given by values of Q approaching infinity and a phase difference G of 90°.

4.1. *Equivalent barotropization by β*

In Figs. 1a, b, the difference in the structural quantities between the f- and β-plane runs (except for the inviscid cases) are presented for the first 10 zonal wave components of the gravest

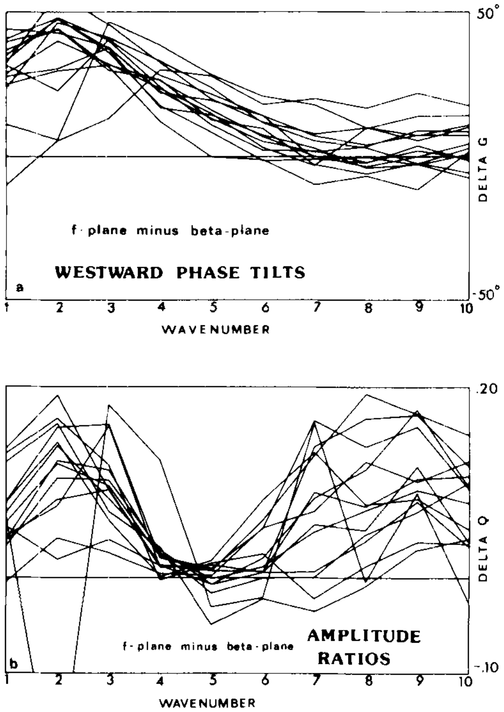

Fig. 1. The influences of β upon the statistically equilibrated states. Differences between the numerically simulated (a) phase difference G, and (b) amplitude ratio Q, for each of the f-plane and β-plane experiments for the first 10 zonal components of the gravest meridional wave modes (the wavenumbers are increasing to the right). The horizontal axes that divide the plots denote the zero line with positive values above and negative values below. Positive values of each quantity indicate that the value is greater on the f-plane.

meridional mode. (Though this selection represents only 10 out of 441 wave components, almost all of the energy resides in the 10 components selected for presentation.) Fig. 1a contrasts the G values and 1b the Q values. Positive values indicate that the f-plane quantities exceed the corresponding β-plane quantities.

The figures clearly demonstrate that the longer waves (wavenumbers less than 5), in all the runs that could be contrasted, are strongly barotropized by the β-effect, especially in the case of the phase differences. On the f-plane, the temperature field of the longest waves lags the streamfunction field by 25° to 50° more than the corresponding structures on the β-plane, and since G itself in both cases is always less than 90°, the f-plane disturbances have much greater westward phase tilts with height. The amplitude ratio Q is also larger on the f-plane, though there is considerable scatter in individual comparisons, indicating a relatively greater thermal to streamfunction component. Since $Q \sin G$ is proportional to the poleward heat transports, the disturbances are clearly structurally more efficient on the f-plane than the β-plane.

The barotropizing effects of β are also reflected in the time-average gravest mode zonal jet component shown in Fig. 2. The vertical-axis represents the contribution by the gravest mode zonal component to the speed of the jet at the center of the channel ($y = \pi L/2$) at 500 mb (m s^{-1}). The horizontal-axis has no physical interpretation; it is simply ordered by the speed of the zonal flow for the various runs on the f-plane. The lower line represents the zonal wind speeds on the f-plane, and the upper line the zonal wind speeds for the same parameter set but on the β-plane. The abbreviations next to selected circles correspond to the parameters as given in Table 1. In all cases, β leads to a substantial increase in the zonal flows consistent with the decreased efficiencies of the corresponding waves.

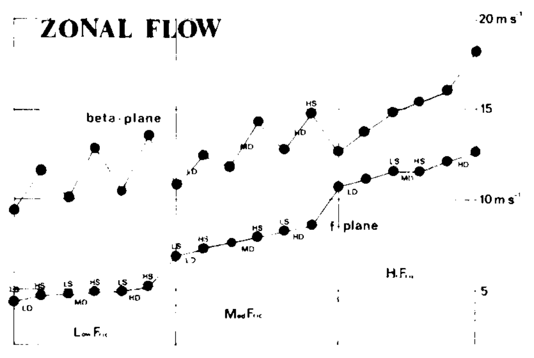

Fig. 2. The zonal wind speed (m s^{-1}) due to the gravest zonal mode component at 500 mb at the channel center for the f- and β-plane runs. The circles on the upper line are from the β-plane while those on the lower line are from the f-plane. The two circles which have the same "x-value" or horizontal-axis value differ only in the β parameter. The abbreviations next to the circles denote the parameter set according to Table 1.

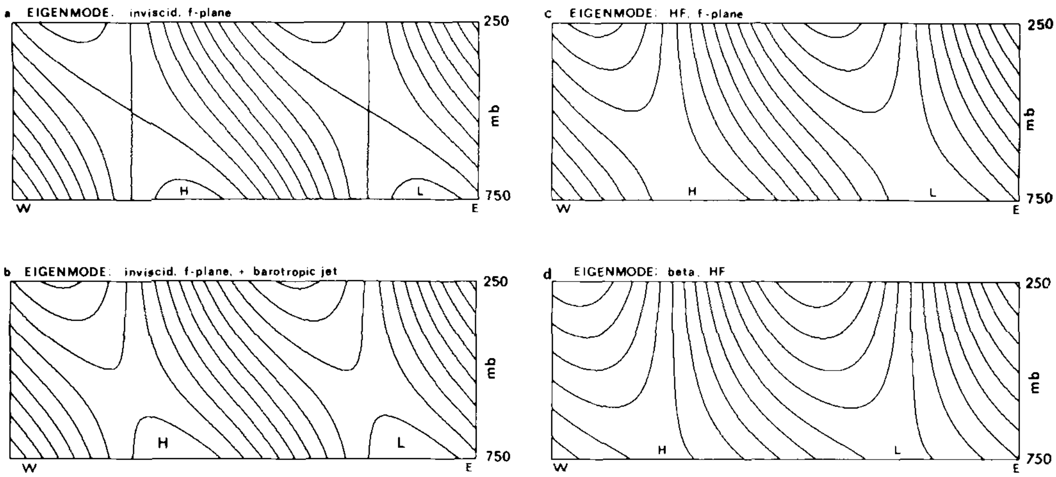

Fig. 3. The "continuous" vertical structure of selected eigenmodes in the two-layer model interpolated for all levels. The temperature perturbation is assumed to be at $x = 0$ or $2\pi L/nk$. The x-axis ranges from zero to $2\pi L/nk$, where k is the zonal wavenumber and the y-axis ranges from the lower level (750 mb) to the upper level (250 mb). (a) The eigenmode calculated in the absence of dissipation, on the f-plane, and without a barotropic component of the zonal flow, (b) The same as (a), except that a barotropic component of the zonal flow has been added such that the lower-level zonal flow is zero, (c) The same as (b) that except dissipation has been added equivalent to the high dissipation parameter set; (d) The same as (c) except for the addition of β.

4.2. Two-layer model vertical structures

At this point, it is advantageous to clarify that linear dynamics, even in a two-layer model, can do a respectable job of representing realistic disturbances, primarily via the inclusion of the parameter β and the other equivalent barotropizing mechanisms (such as asymmetric friction, i.e., different values of the friction at the top and bottom layers, and shears in the horizontal winds; see R). These parameters play an important rôle in the establishment of qualitatively atmospheric-like equivalent barotropic structures that has often been attributed to other processes. It is generally considered that the vertical resolution in the two-layer model is too coarse to generate disturbances whose vertical profiles are somewhat reminiscent of reality. This assumption is incorrect, and has most likely evolved from the analysis of the baroclinic eigenmodes that develop upon idealized zonal basic states consisting of only vertical shear. The addition of β into the problem completely modifies the structures obtained in the f-plane case to something which appears quite reasonable, even in a two-layer model.

Using the height-independent thermal wind of the two-layer model, a stream-function amplitude can be linearly interpolated for all levels. If the temperature perturbation is assumed to have an absolute phase of zero, the amplitude of an arbitrarily specified wave structure in the two-layer context at any level can be obtained from

$$\psi(p, x) = \Psi\sqrt{1 + p^2 Q^2 + 2Qp \cos G} \times \cos(nmx - D),$$

where

$$D = \tan^{-1}[\sin G/(\cos G + pQ)]$$

and Q and G are the non-dimensional amplitude ratio and phase difference between the thermal and stream-function components, respectively, Ψ is an arbitrary amplitude factor, and p is the level, where $p = -1$ corresponds to the lower layer and $p = 1$ corresponds to the upper layer. The structures of four different eigenmodes are then plotted in Figs. 3a–d.

Fig. 3a is the classic structure in the inviscid case with a zonal basic state consisting of a purely vertically sheared sinusoidal jet (thus easterlies at the lower level with equal magnitude westerlies at the upper level) and a specified static stability. Fig. 3b is the eigenmode for the same conditions except that a zonal sinusoidal barotropic jet has been added to the basic state

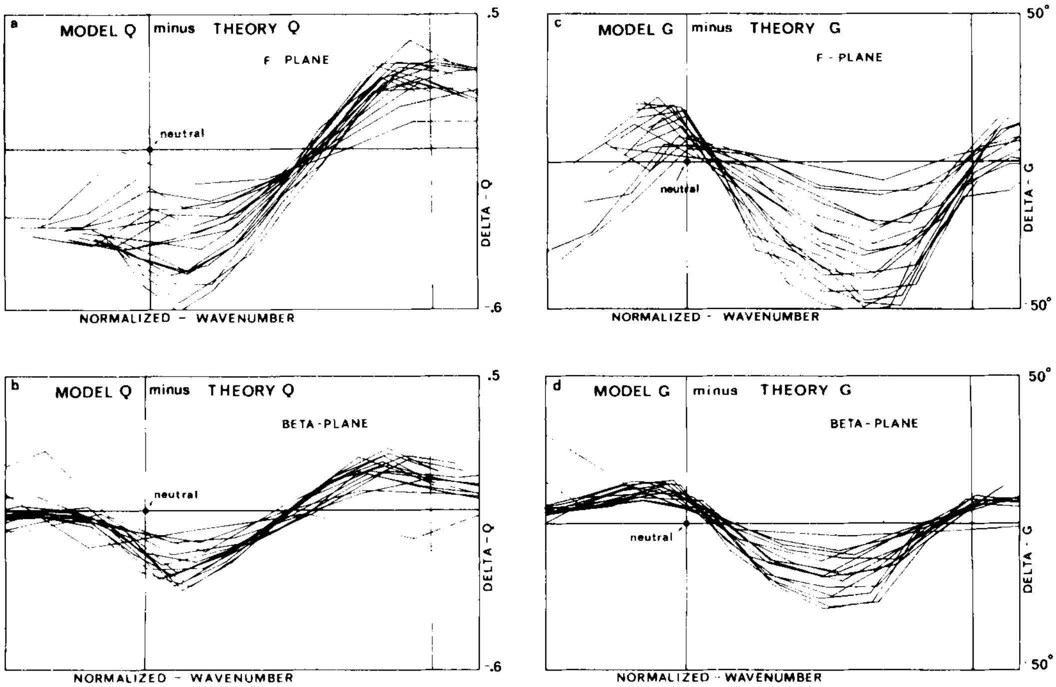

Fig. 4. The differences between the numerically simulated structures and the eigenmodes computed from the time-averaged gravest mode zonal flow of the high-resolution model. The horizontal axes have been normalized by the growth rate such that the vertical lines to the left and right in each figure denote the marginal curves. Thus the total number of wavenumbers contained in the traditionally unstable region between the two lines may be different for each experiment. The horizontal lines subdividing the figure are the zero axes. Positive values lie above the lines and occur when the numerically simulated values exceed that of the eigenmode. (a) The differences in the amplitude ratio Q on the f-plane; (b) The same as (a) but on the β-plane; (c) The differences in G on the f-plane. (d) The same as in (c) but on the (β) plane.

such that the flow at the lower layer is zero. (If the zonal basic state were chosen such that the winds were constant in the meridional direction, instead of being a sinusoidal jet, Fig. 3b would look the same as Fig. 3a.) Fig. 3c is the same as the preceding case except dissipation, corresponding to the high friction (HS) values in the previous experiments, has been added, and Fig. 3d is the same as 3c except for the inclusion of β.

The vertically symmetric, nearly straight-line tilt of the trough and ridge axes (in no case is it ever a completely straight line as is often erroneously assumed in two-layer models) of the simplest inviscid case is the structure obtained in the Eady model (see Fig. 7.72 of Pedlosky (1979)). This structure of maximum amplitude at the lowest and highest levels is often associated with idealized (theoretical) baroclinic perturbations, though it is not very representative of typical atmospheric structures. On the other hand, when (asymmetric) dissipation and β are added to the parameters, the consequent structures are much more representative of the disturbances considered typical in the atmosphere. It is often assumed that a continuous type of construction, such as the Charney (1947) model, is required to develop the equivalent-barotropic amplitude profiles and sloping trough and ridge axes that are shown in Fig. 3d. However, it is clear that the two-level model captures the qualitative features of these disturbances. It may also be likely that the β effect, which is included in the Charney model, is responsible for the aesthetically pleasing vertical profiles of the eigenmodes and not the vertical continuity of the basic state. On the other hand, the lack of vertical resolution in the two-layer model is responsible for the inability of the model to develop the shallow layers of low-level, low static stability that lead to the unstable short-wave (wavenumber 12–15) disturbances with maximum amplitude at the surface, as shown by Staley and Gall (1977) and Blumen (1979).

4.3. Theoretical versus numerical structures

The numerical simulations presented above strongly support the notion that the spherical geometry of the earth is a principal factor behind the equivalent barotropic structures of the equilibrated atmospheric long waves. Of course, there is no a priori reason to assume that β is operating in the same manner in the numerical model as in the model of R, even if it is evident that β is a major element in determining the equivalent barotropic structures of the equilibrated disturbances and the zonal flow speeds in the numerical simulation. Our point is that the *equivalent* barotropization is due primarily to the linear modification of baroclinic structures by the parameters, in contrast to the concept proposed by Salmon (1980) that the downscale shift of the baroclinic energy input by β allows more room in spectral space for the barotropic processes to ensue.

A measure of the degree to which the simple structural determinism ideas account for the numerically simulated structures (and thus one's understanding of them) can be estimated by contrasting the numerical structures with those given by the eigenmodes that develop upon the time-averaged zonal flows. If the wave-wave (and other) interactions present in the more sophisticated model do not influence the structures at all, the eigenmodes and numerically simulated disturbances will be identical.

However, the time-averaged zonal flow contains higher-order meridional components which are unaccounted for in the simple model of R. Even though these higher-order meridional components are more than an order of magnitude smaller than the gravest-mode component, the consequent structures driven by the full zonal flow would be capable of transporting momentum as well as heat. Thus, a more appropriate comparative study would result from the extension of the model of R to include multiple meridional modes such that the momentum transports could also enter into the nonlinear balances. In the absence of such a theory, only the *gravest* mode component of the time-average zonal flow is used as a basic state in the stability analysis.

These comparisons are then shown in Figs. 4a–d (except for the inviscid cases), which present the difference between the "linearly" (quotes are placed here since *nonlinear* processes are involved in the establishment of the time-averaged basic state) and numerically determined gravest meridional mode wave components. Fig. 4a presents the differences of the amplitude ratio on the f-plane, 4b the same on the β-plane, while 4c and 4d contrast the phase differences on the f- and β-planes, respectively. (Positive values indicate that the numerical calculations exceed that of the eigenmode.) In addition, the horizontal-axis has been scaled by the corresponding growth rate curve such that the left- and right-most vertical lines denote the *wavenumber* of *marginal stability* for the numerically-simulated time-averaged zonal flow.

The figures demonstrate two noteworthy features. First, the discrepancies between the one-wave theory and the numerical simulations exhibit a clear relation to the growth rates (instead of the actual scale of the waves) and second, the dependence of the discrepancies upon these growth rates is *systematic* for all the experiments, i.e., they possess a similar shape and vary primarily in magnitude. The first result is perhaps to be anticipated since the theoretical conditions for equilibration in R require a zero growth rate, and thus the deviation of the growth rate from zero provides some measure of the influence of the wave-wave interactions upon the structures over those determined by the processes considered in R alone. However, the analysis is not quite so simple, for if that were the case, the theoretical and numerically simulated structures would be most reminiscent of one another at the marginal curves and most unlike one another at those points where the growth rate is a maximum or minimum (most negative). Though this is the case for the phase differences G, the opposite is true for the amplitude ratios Q. But in either case, the dependence of the discrepancies upon the growth rates *instead* of the actual wavenumber, indicates the strong influence of baroclinic processes upon the equilibration.

The *systematic* behavior of the discrepancies as a function of the growth rates further indicates the importance of structural determinism. Even though an individual case may be significantly modified by the organized transports due to the wave-wave interactions that the simple model does not account for (equilibration process number two of Salmon, 1980, Vallis, 1988), the modification by these unaccounted-for processes is systematic through parameter space. Consequently, if one changes a given parameter, such as β, the effects upon the equilibrated flow due to this parameter *change* can be, to a reasonable extent, anticipated by examination of the structural changes the given parameter will induce in the one-wave model example. Note that we could *not* draw the same conclusions if the discrepancies were not systematic and growth-rate dependent (and were of similar magnitude, of course). A chaotic scatter of the discrepancies about the growth rate curves (which occurs in the two inviscid runs) might be anticipated if turbulent scrambling processes dominated the equilibration dynamics (process number three of Salmon (1980), Vallis (1988)).

The equivalent barotropization due to β in these strongly forced and dissipated models then appears to be much more a consequence of the influence β exerts upon the structures than Salmon's down-scale shift hypothesis. If the latter were the case, one would expect not only the barotropization, but a shift in energy upscale in going from the f- to β-planes, as more "room" in spectral space is created. In strongly structurally deterministic situations, this behavior is not observed. The energy maximum tends to follow, instead, the marginal curve (which can be seen in Fig. 6 and is discussed in detail in Subsection 4.4). The marginal curve, meanwhile, shifts to smaller scales with the addition of β.

Perhaps an even more potent demonstration of the rôle of structural determinism upon the equilibration is provided by the examination of the equilibration spectra as a function of the static stability. No other single parameter in the model exerts such a strong influence upon the scale of the most unstable wave than this parameter. Consequently, one would expect to see a significant increase in the barotropization and a *strong upscale* shift of the energy maxima for *decreases* in the static stability parameter, which markedly shifts the wave of maximum instability to shorter scales (see Figs. 1 or 6 of R). However, on the f-plane, the spectra and zonal flows (the latter of which can be seen in Fig. 2) are almost completely insensitive to this parameter. A closer examination of the structural influences due to this parameter reveals that the energy-containing longer waves in the vicinity of the marginal curve are nearly independent of the static stability (see Fig. 6b of R); thus the influence upon the equilibrated state is minor. A similar degree of insensitivity is not quite the case on the β-plane, as the energy-containing longer waves *do* undergo minor structural changes in response to the static stability (primarily due to the downscale shift of the marginal curve on the β-plane), which is reflected by the small increase in the zonal flows in Fig. 2 between the LS to HS cases. The important point is that the *equilibrium statistics appear to be most sensitive to the overall changes in the induced structures* rather than the shift of energy input scale. Otherwise, decreasing the static stability parameter would be an even more effective means of barotropization, as it is much more effective at transferring the scale of the most unstable disturbances to smaller scales than increasing β.

The systematic and deterministic nature of the numerical model structures also indicates that the evolution of the thermal and stream-function components to their preferred arrangements is quite robust. If one views the balance as the thermal field adjusting to the streamfunction field, a partial explanation for Held's (1983) question "Why do barotropic models work as well as they do?" ensues. In strongly structurally deterministic flow situations, the thermal and vorticity fields rapidly adjust to a preferred structure. In a statistically equilibrated state in which no sudden inputs of energy from the release of baroclinic instability are occurring, the baroclinic processes are then primarily engaged with the barotropic mechanisms to establish specific structures. Consequently, the barotropic prediction of the vorticity fields (to which the thermal fields adjust) is quite successful at time scales long compared to the adjustment time of the structures.

The final important note comes from the results of the two inviscid runs, which are completely different than any of the remaining forced-dissipative experiments. First, there is little difference between the β- and f-plane runs:

the overwhelming majority of the wave energy is in the largest-scale component, and the zonal shear is nearly zero, while the barotropic zonal flow is about the same as the initial value. Second, the phase differences for all the components are essentially zero. In short, the system has become barotropic, and not equivalent barotropic. Here the effects of turbulence clearly dominate, as the inviscid case is structurally indeterministic as the flow becomes baroclinically neutral (see R).

4.4. The amplitudes

In the state of statistical equilibrium, each component of the numerical model must be receiving as much energy as it is losing. The energy sources (or sinks) at each scale are accomplished by transfers to or from other wave components and zonal flows, while dissipation is always a sink. The magnitudes of these various transfers are determined by the amplitude and phase relations between all the components present in the equilibrated state. In the simple one-wave theory, only the transfers between the gravest mode zonal flow and the wave component are involved in determining the equilibrated amplitudes. The question is to what degree this single process influences the level of amplitude equilibration of each component in the numerical model in the presence of all the remaining transfer processes, both organized and turbulent; in particular, in determining at which scale the energy will be a maximum.

Since the "energy spectra" of the one-wave model consists of only one component, the only manner in which a "spectra" of the one-wave model can be generated is to compute the equilibrium energy as a function of wavenumber. As stated previously, the maximum of this artificially generated spectra will not necessarily occur at that wavenumber which is traditionally most unstable, but either on the long- or short-wave side of it (or both). To provide a qualitative measure of the degree to which the equilibrium dynamics of the one-wave model (which involves only heat-transport efficiencies) is still present in the numerical model, the scale at which the artificial spectrum obtains its maximum is contrasted with the peak in the spectrum of the corresponding numerical model as a function of the external parameters.

These comparisons are provided by Figs. 5a–d, which contrast the equilibrated amplitude of the one-wave model (thin curvy lines) as a continuous function of wavenumber (increasing to the right) and thermal driving θ^* (increasing downward), for four of the remaining parameter combinations in Table 1, with the wavenumbers in the corresponding numerical model runs which have the highest energies. The discrete wavenumbers allowed in the numerical model are indicated along the x-axis, while the 3 values of the thermal drivings used in the 36 runs are denoted by LD, MD, and HD as in Table 1. The heavy line indicates the location of the one-wave model long-wave maxima, while the solid circles indicate those discrete wavenumbers in the numerical experiments that have the highest energies. Since the 21×21 wave runs are limited by the discrete property of the periodicity requirement, to better obtain a sense of the shape of the spectra in the vicinity of the maxima, an asterisk is provided to indicate which scale has the second-highest energy. If two waves are nearly tied for second place, both are shown by asterisks. The parameter sets are (a) high-friction, high static stability, β-plane, (b) low-friction, low-static stability, f-plane, (c) high-friction, low static stability, β-plane, and (d) as in (a) but on the f-plane.

The comparisons demonstrate some qualitative success in the sense that the shift in the location of the numerical model energy maxima follows the shift in the long-wave maxima of the theory, in spite of the fact only the organized largest-scale component of the heat transports are accounted for. Again, as in the case of the structures, predictions of the changes in the locations of the energy maxima for changes in the external parameters are most successful, whereas the absolute quantitative location of the maximum for a single case is not as well identified. A distinct discrepancy is, however, that no secondary short-wave maximum is found in the numerical model, which can be rather easily explained by Salmon's (1978) results.

In this perspective, then, the location of the energy maximum at scales larger than the most unstable modes appears to be partially accounted for by the structural efficiency and poleward heat-transport balance arguments in the following manner: though the traditionally most unstable wave amplifies most rapidly in the linear

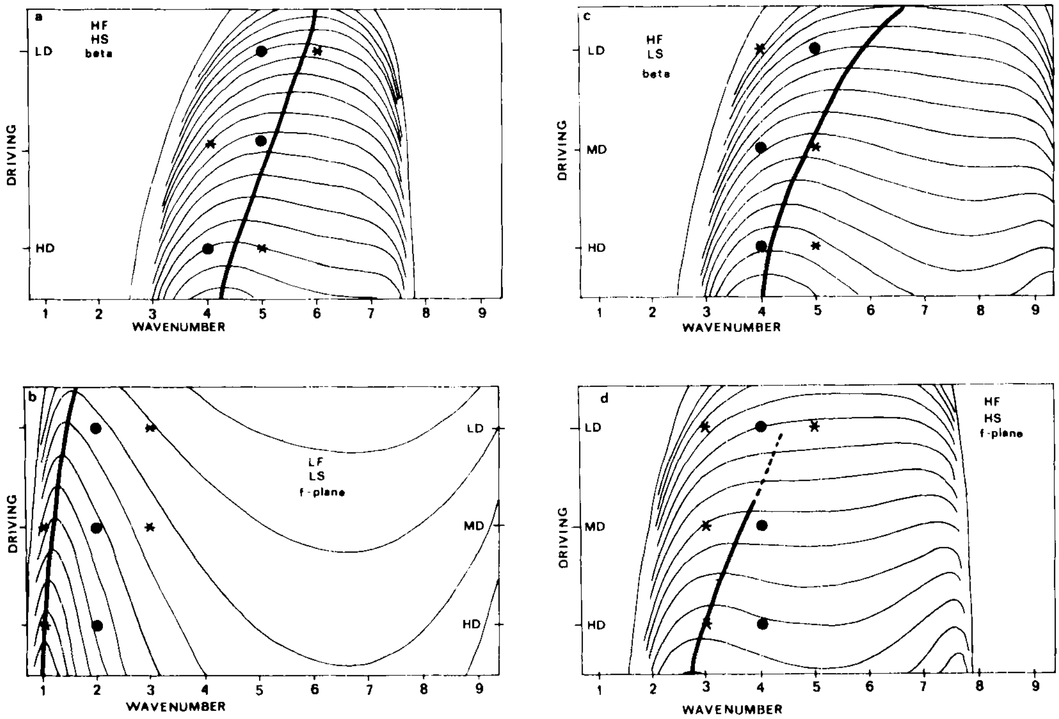

Fig. 5. Comparison of the numerically simulated amplitude maxima for selected high-resolution runs with the amplitudes of the analogous one-wave model. The horizontal axis represents the wavenumber ratio n (increasing to the right), where the integer values then denote the locations of the allowable waves in the numerical model (kn for $k = 1, 2, \ldots$). The vertical axis is the driving θ^* (increasing downward) where the low, middle, and high values of the driving used in the experiments are denoted. The thin curves are the amplitudes of the one-wave model while the heavy curve marks the approximate location of the long-wave, one-wave model amplitude maxima. The solid circles indicate the observed wavenumber that had the largest energy in the multi-wave model. The asterisks denote the waves of second-largest magnitude (2 asterisks appear if the second-largest amplitudes were about equally divided between 2 components). The parameter sets displayed are (a) high-dissipation, high-static stability, β-plane; (b) low-dissipation, low static stability f-plane; (c) high-dissipation, low-static stability β-plane; (d) high-dissipation, high-static stability, f-plane.

regime, it is very effective at transporting heat poleward and does not require a large amplitude to equilibrate with a given zonal flow. The remaining waves, on the other hand, are much less efficient and require substantially larger amplitudes before they can equilibrate with a given zonal flow and thus continue to amplify. At larger scales, enough signal remains from this process that the one-wave theory can qualitatively locate the numerical model's energy-spectra maxima, whereas at smaller scales, the equilibration mechanism is swamped by the remaining transfer processes between the waves and chaotic scrambling.

The larger amplitude of the longer waves in combination with their structurally deterministic preferred configurations, probably enhances the aforementioned manner of equilibration over that of the other processes listed by Salmon (1980), in particular, that of scrambling. Homogeneous scrambling of disturbances disrupts the correlation between the thermal and vorticity fields necessary for energy extraction, cutting off any growth, even though the zonal flows may still be linearly unstable. The smaller scale disturbances are more influenced by a given level of scrambling than the larger-scale disturbances, as the smaller-scale disturbances possess higher values of the enstrophy, leading to more effective scrambling. Clearly, some process enhances the rate of equilibration of the shortest waves in the numerical model, for they are still linearly unstable with respect to the gravest mode mean zonal jet, yet do not amplify. How much of this equilibration is due to scrambling or organized, structurally determined transports that we have not accounted for, is unknown.

We also must point out that following the one-wave model *precisely* would predict an equilibrated state with just one wave: that which requires the minimum vertical shear to amplify, which would be the case if wave-wave interactions were removed (as in Mak (1985) and Vallis (1988)). The fact that energy is transferred between the different waves and turbulent scrambling is present drives supercritical zonal flows and establishes the presence of other waves. These waves are then forced into certain configurations (part of which we can account for: the wave-mean flow interactions; and part which we cannot: the wave-wave interactions) which are furthermore disrupted by scrambling. Our point is that to accomplish the required transports for balance, larger amplitudes are necessary for more inefficient structures. From our experiments, it appears that the structural contribution due to wave-mean flow interactions and the feedbacks determined by that structure still have a significant signal at the larger scales.

Even though the success of the one-wave model is quite limited, the runs *do* indicate that the equilibrated state is strongly controlled by structural determinism. One consequence of this equilibration process is that the energy maximum should lie in the vicinity of the marginal curve. This behavior is clearly seen in Fig. 9 of Haidvogel and Held (1980). In Fig. 6, the energy maxima for the experiments are plotted relative to the normalized growth rates in the same manner as in Fig. 4. The locations of the maxima are denoted by dots, where the dots in the lower half are from the f-plane results while those in the upper half are from the β-plane (the left-most dot and open circle from the β-plane case are from the same run, the latter being a secondary maximum). The long-wave marginal curve is given by the vertical line to the left while the short-wave analogue appears to the right, almost at the border of the figure. Though not as clean as Haidvogel and Held's (1980) result, a clear tendency for the maxima to cluster about the marginal point is evident. The rôle of structural determinism is also evident, as the cases which lie furthest to the left are those with the smallest amounts of dissipation and most structurally indeterministic, and thus tend towards behaviors more in accord with turbulence theory, and vice versa (in the inviscid runs, the largest-scale component has the overwhelmingly largest energy). The structurally destabilizing influence of β is also reflected in the leftward shift of the maxima *relative* to the marginal point, even though in all cases but one, the *actual* wavenumber of the energy maximum *increases* upon the addition of β. Both the processes of structural determinism and homogeneous turbulences are clearly present in these runs, the latter becoming more significant as the inviscid, homogeneous environment is approached.

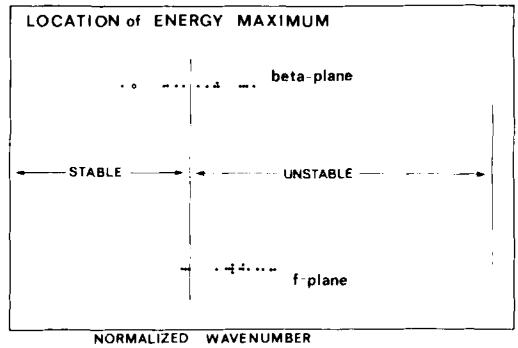

Fig. 6. The location of the energy maxima relative to the marginal stability curves (denoted by the 2 thin vertical lines); in other words scaled as in Fig. 4. The β-plane runs are plotted in the upper part of the figure and the f-plane results in the lower part. Note the concentration around the point of long-wave marginal stability, and the relative shift of the β-plane results towards long-wave stability. The linearly most unstable wave, on the other hand, tends to lie on the short-wave side of the center of the denoted unstable region.

Even if the one-wave theory can provide a partial explanation for the location of the energy peak in the numerical model, the numerical model spectra do not reproduce an energy spectra that is considered typical of the atmosphere. In the majority of the numerical simulations, a well-defined peak in the energy occurs at a scale considerably smaller than the largest scale resolvable in the model. In fact, for those parameter sets which otherwise generate zonal flows and disturbance amplitudes that synoptically best simulate the atmosphere, the energy peak occurs at wavenumbers 4 or 5. Part of this inconsistency appears to be due to the complete absence of zonally inhomogeneous external forcing mechanisms (such as topography) in the numerical model.

This suspicion is supported by the spectra generated from the rotating basin experiments of Li et al. (1986) with and without a wavenumber-2 topography. In the absence of topography, the form of the spectrum obtained by Li et al. (1986) (their Fig. 7) is similar in several quantitative respects to the spectra obtained in the high-resolution model; in particular, the distinct energy peak at some scale smaller than the largest scale (in their case at wavenumber 6) as well as the weak secondary maximum at the largest scale. In their experiment with topography, Li et al. (1986) find that much more of the energy is channeled into the large-scale harmonics of the topography, producing a significantly flatter distribution than their no-mountain experiment.

Examination of just the *transient* component of the atmospheric spectrum (Fig. 1a of Boer and Shepherd, 1983) further suggests that the free atmosphere would tend to develop a more peaked spectrum as in the numerical model if the orography could be removed. More solid observational evidence for the topographic distortion of the energy spectrum is provided by the work of Salby (1982). His analysis of Southern Hemisphere FGGE data shows a distinct and dominating energy peak at wavenumber 5 that appears *only* during the summer season. The rôle of topography is suspected to be at a minimum during the Southern Hemisphere summer as the jet has reached its southern-most extent maximizing its transit over the oceans. The peaking of the numerical model spectra appear, then, not to be a failure in the dynamics, but perhaps represents the type of spectra the atmosphere would obtain if the wave structures were not influenced by zonally inhomogeneous boundary forcings.

5. Summary

The results of the numerical experiments clearly demonstrate that the β-effect is one of the principal means for establishing equivalent barotropic structures and high zonal flow speeds. The larger scale disturbances in the f-plane analogues have much greater westward phase tilts with height and, at almost all scales, an enhanced baroclinic component (and thus greater poleward heat-transport efficiencies leading to markedly reduced zonal flow magnitudes) with respect to the β-plane runs. Comparisons between the eigenmode structures computed utilizing the time-averaged gravest zonal mode flow of the numerical model as a basic state with those generated numerically, are consistent with the concept that the equivalent barotropization by β occurs through the same dynamical process of asymmetric influence upon the vorticity and thermal advections as in the one-wave model. The idea proposed by Salmon (1980) that barotropization occurs as the baroclinic energy input source moves downscale allowing more room in spectral space for the homogeneous turbulence concepts to apply, seems to be swamped by the occurrence of preferred structures in our model.

In the atmosphere, the rôle of structural determinism is clearly much more complicated, as zonally inhomogeneous sources of external forcing lead to nonzonal time-averaged states. Both the forcings and the non-zonal time mean states modify the determined structures in manners which are currently poorly understood. Disturbances then possess not only preferred vertical configurations, but horizontal modulations such as storm tracks, which, through their feedbacks, can lead to features such as weather regimes. This more general interpretation of structural determinism appears to be consistent with the work of Shepherd (1987). The organization of the baroclinic disturbances into preferred configurations determines the consequent feedbacks and transports, modifying and biasing the scrambling effects of pure turbulence.

Though the numerical model is not the atmosphere, the robustness of this influence by β in the quasi-geostrophic model strongly suggests that the spherical geometry of the earth, through similar means, is a major factor behind the equivalent barotropic structure and zonal flow speeds of the statistically equilibrated flow. The common practice of applying barotropic physics to simulate the atmosphere would probably be much less popular if the earth were on an f-plane, due to the occurrence of much greater westward vertical phase tilts. On the other hand, the deterministic nature of the structures would probably give rise to an equally as effective handling by barotropic physics as on the β-plane.

A partial explanation for the large-scale energy distribution also appears to be provided by the structural efficiency- (heat transport) zonal driving balance argument elucidated by the one-wave model, though it is clear that there are several deficiencies. In spite of the host of wave-wave energy transfer processes in the numerical model, both organized and turbulent, enough signal remains from the zonal flow-wave transfer process of the one-wave model that it is able to qualitatively locate at which scale the energy tends to maximize. Consequently, in the crudest qualitative sense, the establishment of the energy into the larger scales distinct from those scales which are traditionally most baroclinically unstable, is a result of the lowered efficiency of these waves, which then must attain greater amplitudes in order to transport a given amount of heat poleward. (From another point of view, the degree to which the one-wave model describes the location of the energy maximum is a measure of the degree to which Stone's (1978) baroclinic adjustment is applicable.)

We do not mean to imply here that turbulence processes are unimportant, but that they are modified by the occurrence of preferred structures, the latter of which *only* arise in forced-dissipative systems. Preferred structures imply preferred feedbacks which bias the statistically homogeneous feedbacks present in geostrophic turbulence. Though a matter of taste, we view the structural determinism concepts as conceptually advantageous, since one can understand equilibration as a consequence of specified disturbances (which are easy to picture) instead of a statistical ensemble. The price one pays, of course, is that it is currently very difficult to understand the details of how a given structure arises, even in very simple contexts. Full understanding of statistical equilibrium in forced-dissipative systems will require the understanding of both the influences of turbulent scrambling as well as the details of structural determinism, which together determine the nonlinear feedbacks.

6. Acknowledgments

Thanks are given to Erland Källen for his many contributions in this work. One of the reviewers, Geoff Vallis, as well as Theo Shepherd were also of great help with their contributions in the turbulence field. The research was supported by the Swedish Natural Research Council (NFR), contract G-GU1705-108, and the American National Science Foundation (NSF), grant ATM8305295. Additionally, computer time was provided by the Swedish Meteorological and Hydrological Institute (SMHI).

REFERENCES

Baer, F. 1972. An alternate scale representation of atmospheric energy spectra. *J. Atmos. Sci. 29*, 649–664.

Baer, F. 1974. Hemispheric spectral statistics of APE. *J. Atmos. Sci. 31*, 932–941.

Blumen, W. 1979. On short-wave baroclinic instability. *J. Atmos. Sci. 36*, 1925–1933.

Boer, B. J. and Shepherd, T. G. 1983. Large-scale two-dimensional turbulence in the atmosphere. *J. Atmos. Sci. 40*, 164–184.

Charney, J. G. 1947. The dynamics of long waves in a baroclinic westerly current. *J. Meteor. 4*, 135–162.

Deland, R. J. 1973. Spectral analysis of traveling planetary scale waves: Vertical structure in the middle latitudes of Northern Hemisphere. *Tellus 25*, 355–373.

Dole, R. M. 1986. Persistent anomalies of the extratropical Northern Hemisphere wintertime circulation: Structure. *Mon. Wea. Rev. 114*, 178–207.

Gall, R. L. 1976a. A comparison of linear baroclinic instability theory with eddy statistics of a general circulation model. *J. Atmos. Sci. 33*, 349–373.

Gall, R. L. 1976b. Structural changes of growing baroclinic waves. *J. Atmos. Sci. 33*, 374–390.

Gall, R. L., Blakeslee, R. and Somerville, R. C. 1979. Baroclinic instability and the selection of the zonal scale of the transient eddies of middle latitudes. *J. Atmos. Sci. 36*, 767–784.

Haidvogel, D. B. and Held, I. M. 1980. Homogeneous quasi-geostrophic turbulence driven by a uniform temperature gradient. *J. Atmos. Sci. 37*, 2644-2660.

Held. I. M. 1983. Stationary and quasi-stationary eddies in the extratropical atmosphere: Theory. In *Large-scale dynamical processes in the atmosphere* (eds. B. J. Hoskins and R. P. Pierce). New York: Academic Press, 397 pp.

Lau, N.-C. 1979. The observed structure of tropospheric stationary waves and the local balances of vorticity and heat. *J. Atmos. Sci 36*, 996–1016.

Li, G.-Q., Kung, R. and Pfeffer, R. 1986. An experimental study of baroclinic flows with and without two-wave bottom topography. *J. Atmos. Sci. 43*, 2585–2599.

Lorenz, E. N. 1963. Mechanics of vacillation. *J. Atmos. Sci. 20*, 448–464.

Machenhauer, B. and Rasmussen, E. 1972. On the integration of the spectral hydrodynamical equations by a transform method. *Report no. 3*, University of Copenhagen, Institute for theoretical meteorology, 42 pp.

Mak, M. 1985. Equilibration in nonlinear baroclinic instability. *J. Atmos. Sci. 42*, 2764–2782.

Orszag, S. A. 1970. Transform method for the calculation of vector-coupled sums: Application to the spectral form of the vorticity equation. *J. Atmos. Sci. 27*, 890–895.

Pedlosky, J. 1979. *Geophysical fluid dynamics*. New York: Springer-Verlag, 626 pp.

Reinhold, B. B. 1986. Structural determinism of linear baroclinic waves and simple nonlinear equilibration. *J. Atmos. Sci. 43*, 1484–1504.

Reinhold, B. B. and Pierrehumbert, R. T. 1982. Dynamics of weather regimes: Quasi-stationary waves and weather regimes. *Mon. Wea. Rev. 110*, 1105–1145.

Rhines, P. B. 1979. Geostrophic turbulence. *Ann. Rev. Fluid. Mec. 11*, 401–441.

Salby, M. L. 1982. A ubiquitous wavenumber-5 anomaly in the Southern Hemisphere during FGGE. *Mon. Wea. Rev. 110*. 1712–1720.

Salmon, R. 1978. Two-layer quasi-geostrophic turbulence in a simple special case. *Geo. Astro. Fluid Dyn. 10*, 25–52.

Salmon, R. 1980. Baroclinic instability and geostrophic turbulence. *Geo. Astrophy. Fluid Dynamics. 15*, 167-211.

Shepherd, T. G. 1987. A spectral view of nonlinear fluxes and stationary-transient interaction in the atmosphere. *J. Atmos. Sci. 44*, 1166–1178.

Simmons, A. J. and Hoskins, B. J. 1978. The life cycle of some baroclinic waves. *J. Atmos. Sci. 35*, 414-432.

Simmons, A. J. and Hoskins, B. J. 1980. Barotropic influences on the growth and decay of nonlinear baroclinic waves. *J. Atmos. Sci. 37*, 1679–1684.

Staley, D. O. and Gall, R. L. 1977. On the wavelength of maximum baroclinic instability. *J. Atmos. Sci. 34*, 1679–1688.

Stone, P. 1978. Baroclinic adjustment. *J. Atmos. Sci. 35*, 561–571.

Vallis, G. K. 1985. On the spectral integration of the quasi-geostrophic equations for doubly-periodic and channel flow. *J. Atmos. Sci. 42*, 95–99.

Vallis, G. K. 1988. Numerical studies of eddy transport properties in eddy resolving and parameterized models. Accepted for publ. in *Quart. J. Roy. Met. Soc.*

Washington, M. W. and Parkinson, C. 1986. *An introduction to three-dimensional climate modeling*. Oxford: University Press, 422 pp.